Clays and Clay Minerals, Vol. 44, No. 3, 324–338, 1996.

DIAGENESIS OF OLIGOCENE VITRIC TUFFS TO ZEOLITES, MEXICAN VOLCANIC BELT

LIBERTO DE PABLO-GALÁN[1] AND MARÍA DE L. CHÁVEZ-GARCÍA[2]

[1] Instituto de Geología, Universidad Nacional Autónoma de México, 04510 México, D. F.

[2] Facultad de Química, Universidad Nacional Autónoma de México, 04510 México, D. F.

Abstract—Sedimentary zeolites clinoptilolite, mordenite and erionite occur as diagenetic products of ash falls of rhyolitic composition from the Oligocene Chichindaro Formation at the limits of the Mexican Volcanic Belt with the Mexican Highland. These zeolitic tuffs were formed from open hydrologic environments where rhyolitic glass altered to clinoptilolite + opal-C and to clinoptilolite + mordenite + erionite + opal-C. The process of diagenesis was hydrolysis associated with the removal of SiO_2, K_2O, and Na_2O from the rhyolitic precursor and enrichment of Al_2O_3, MgO, and CaO. The crystallization of clinoptilolite occurs at ratios of SiO_2/Al_2O_3 between 4.91 and 7.14 and $(K_2O + Na_2O)/(MgO + CaO)$ from 2.19 to 0.79. Formation of clinoptilolite appears to be directly from glass and through a vitreous proto-zeolite intermediate. The zeolitic tuff is in contact with a vitric tuff where ash falls were devitrified to K-feldspar and diagenetically altered to smectite + opal-C.

Key Words—Diagenesis, Oligocene Vitric Tuffs, Zeolites.

INTRODUCTION

The La Bufa (Eocene-Oligocene) and Chichindaro (Oligocene) formations are rhyolitic tuffs that are exposed in the southern part of the state of Guanajuato, central Mexico, between the physiographic provinces of the Mexican Highland and the Mexican Volcanic Belt (Ortega et al. 1992). The tuffs are of mineralogical and geochemical interest by virtue of their zeolites and their relation to the precursor pyroclastics, diagenetic fluids and hydrologic environment. The units represent the first discovery of sedimentary zeolites for this part of the country, which is an important industrial, mining, farming and ranching area with relevant environmental problems imposing economic interests on zeolites and their applications. This study presents the mineralogy, geochemistry, petrology and paragenesis of the zeolite deposits. Emphasis will be placed on the reactions involving the transformation of rhyolitic glass to zeolites in an open hydrologic environment and the effects of diagenetic fluids on precursor tuffs.

Previous Work

The geology of sedimentary zeolites have been reviewed by several authors (Hay 1963, 1966, 1977, 1978; Walton 1975; Hay and Sheppard 1977; Surdam 1977; Tsolis-Katagas and Katagas 1989; Altaner and Grim 1990; Sheppard 1991; Lander and Hay 1993). In Mexico, the known localities of sedimentary zeolites are limited to those from the Miocene Suchilquitongo formation in the state of Oaxaca (Wilson and Clabaugh 1970; Mumpton 1973, 1975; de Pablo-Galán 1986) and from the state of Sonora (González-Sandoval 1987; Samaniego 1987). However, the intense Tertiary volcanism that produced extensive deposits of pyroclastics allows the authors to expect more zeolite localities than those presently recognized (de Pablo-Galán 1979). This paper attempts to contribute to the knowledge of zeolites and is based on a study of tuffs from the Oligocene Chichindaro Formation. In addition to its mineralogical and geochemical interest, these zeolites may have economic value because of their cationic selectivity and exchange capacity, which are applicable to industrial processes, agriculture, animal feed and environmental control (Mumpton 1977).

The zeolitic tuffs discussed are located in the southern portion of the state of Guanajuato, central Mexico, between the 20°52′ and 21°00′N latitude and the 101°01′ and 101°19′W longitude. The area of interest covers about 1800 km^2. The tuffs outcrop for 23 km along Highway 45 between the cities of Juventino Rosas and Guanajuato. The tuffs are well exposed along Highway No. 45, the La Trinidad creek, the Cerro del Sombrero and the River Guanajuato. The area is located within the physiographic subprovince of the Bajío Guanajuatense or Guanajuato Lowland in the province of the Mexican Volcanic Belt, limited to the north by the Mexican Highland and to the northeast by the Sierra Madre Oriental. It is characterized by alluvial plains, sierras of low slopes, mesas and basins filled with volcanics (Echegoyen-Sánchez 1970). To the west and northwest of the tuff outcrop are the continental clastics of the Paleocene-Eocene Red Conglomerate and to the south the Quaternary basalts. The area is largely covered by Tertiary lava flows and tuffs of rhyolitic composition and an extrusive sequence of andesite. The Quaternary geology is characterized by lava flows and scoria of basaltic composition. The area is drained by the Guanajuato and La Trinidad rivers flowing NE to SW. Field data suggest that pyroclastic

https://doi.org/10.1346/CCMN.1996.0440303 Published online by Cambridge University Press

material was deposited in a lacustrine environment. Subsequent diagenetic reactions formed the zeolitic tuffs that outcrop at elevations from 1962 to 2182 m (Figure 1).

The oldest rocks in the region, which do not outcrop in this area, are the Esperanza Formation (Triassic-Jurassic) and Las Trancas Formation (Upper Jurassic) (Figure 2). The continental clastics of the Red Conglomerate (Paleocene-Eocene) are overlaid by the tuffaceous sandstone of the Losero Formation (Eocene). The Tertiary volcanic are the welded tuff of the Upper Eocene-Lower Oligocene La Bufa Formation that underlays the rhyolite and tuffs of the Oligocene Chichindaro Formation. The Upper Oligocene consists of the volcanoclastics of intermediate composition of the Calderones Formation, overlaid by the andesite flows of the Cedros Formation that extend into the Lower Miocene. The Miocene faces consist of lava flows and tuffs of rhyolitic composition, covered by Pliocene continental clastics. The Quaternary is characterized by lavas and scoria of basaltic composition (Comisión de Estudios del Territorio Nacional 1973a, 1973b, 1973c; de Csema-Gombos 1975; López-Ramos 1985; Nieto-Samaniego 1990; Consejo de Recursos Minerales 1992).

EXPERIMENTAL

Sampling and Analytical Methods

The zeolitic tuffs were collected at various localities and elevations between the cities of Guanajuato and Juventino Rosas along Highway 45. A total of approximately 100 samples were collected but the analytical data are presented from only those that were the most representative. The localities, stratigraphic units, and lithology are indicated in Table 1.

Thin sections of the bulk samples were studied by optical microscopy utilizing oil-immersion methods to identify the minerals and their paragenesis. The authigenic minerals were identified by X-ray diffraction (XRD) using a Siemens D5000 diffractometer equipped with filtered CuKα radiation, scanning at 1 °2θ/min over the range 4 to 60 °2θ. The clays were solvated by adding ethylene glycol directly to the sample. The relative abundance of minerals was estimated from optical, diffraction and electron microscopy studies. The abundance of clinoptilolite was determined from the intensity of d_{020} = 8.95 Å, using as reference clinoptilolite concentrated with a mixture of bromoform plus acetone from the sampled material. This reference did contain minor glass that could not be loosened by ultrasonic agitation from the intimately associated zeolite. Opal-C was quantified with reference to d_{101} = 4.04 Å, which is broader and less intense for opal than it is for cristobalite devitrified from glass. To differentiate clinoptilolite from heulandite, the samples were heated overnight at 500 °C and analyzed by XRD. Those samples that did not show changes other than minor variations in the intensity of the characteristic peaks were classified as clinoptilolite (Mumpton 1960; Boles 1972; Minato et al. 1985). The chemical composition of the tuffs was determined by X-ray fluorescence (XRF) of pressed powders. The Na and Mg were measured by wet chemistry procedures. Loss of ignition was determined at 850 °C for material previously dried at 60 °C and total Fe is reported as Fe_2O_3. Microtextural relations, crystallization and composition of minerals were determined from flat unpolished specimens by scanning electron microscopy (SEM) coupled with a Kevex energy dispersive spectrometer (EDX) calibrated with rhyolitic glass, feldspar and kaolinite reference materials. The compositions obtained by this technique are considered semi-quantitative, useful in establishing SiO_2/Al_2O_3 and other ratios and to have alternative modes of identification. Infrared absorption spectrometry (IR) was applied to identify adsorbed H_2O, oxhydrils and ionic substitutions. A Perkin Elmer 783 double beam spectrometer was operated at a scanning speed of 1000 cm^{-1}/min from 4000 to 2000 cm^{-1} and at 500 cm^{-1}/min between 2000 and 200 cm^{-1} wavenumbers on material dried at 60 °C and pressed into KBr discs.

RESULTS

Stratigraphy and Lithology

The dominant lithologies for the area are the ignimbrite of the La Bufa Formation, the rhyolite and its tuffs of the Chichindaro Formation, the andesite flows of the Cedros Formation and the Quaternary basalt (Figure 2). They represent an overall thickness of 410 m (Figures 4 and 5).

LA BUFA FORMATION. The Upper Eocene-Lower Oligocene La Bufa Formation is characterized by the welded tuff that crops at elevations from 1772 to 1860 m, 60.7 km SE from Guanajuato on Highway 45, between the town of Juventino Rosas and the crossroad to San Miguel Allende (Figure 1; Table 1, sample 1). It is grayish pink, relatively hard, dense and coarse. Pyroclastic crystals consist of quartz (10%), sanidine (5%), traces of biotite and magnetite in a partially devitrified vitreous matrix. Glass shards represent about 35% of the rock. Glass is devitrified to cryptocrystalline K-feldspar (20%) and opal-C (30%) (Table 2). The composition is rhyolitic with ratios of SiO_2/Al_2O_3 (6.81) and $(Na_2O + K_2O)/(MgO + CaO)$ (7.44), which are similar to those of the overlying Chichindaro rhyolite (Tables 3 and 4). Plotted in the SiO_2/Al_2O_3 versus $(Na_2O + K_2O)/(MgO + CaO)$ diagram this welded tuff groups with other rhyolitic units and discriminates itself readily from the vitric and zeolitic tuffs of the other stratigraphic units (Figure 5). The IR analysis does not show the characteristic H-O-H bend at 1625 cm^{-1} indicative of molecular adsorbed H_2O and dis-

https://doi.org/10.1346/CCMN.1996.0440303 Published online by Cambridge University Press

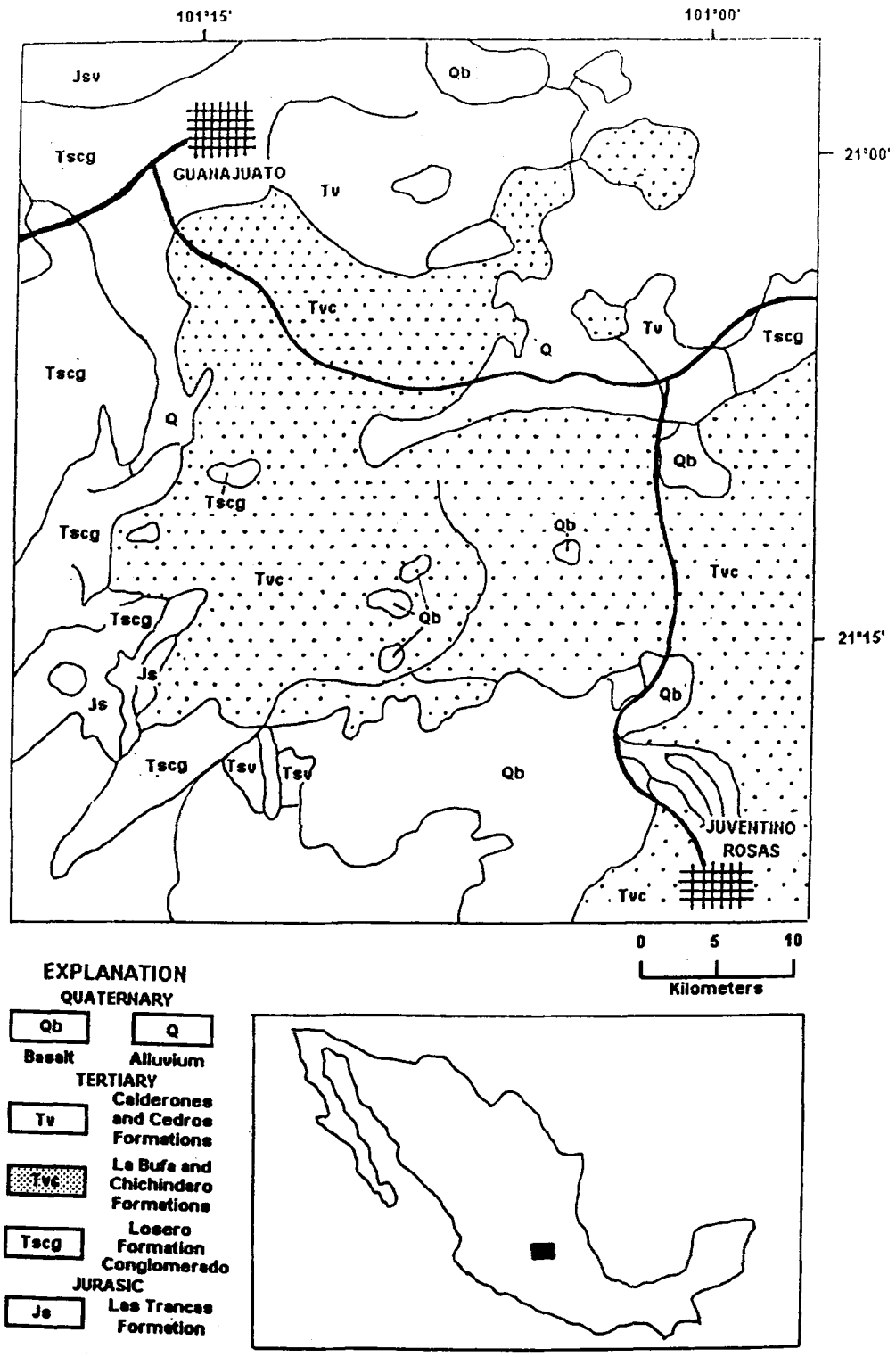

Figure 1. Geologic map showing the area of study in the state of Guanajuato, Mexico, with data taken from Comisión de Estudios del Territorio Nacional (1973a, 1973b, 1973c) and Consejo de Recursos Minerales (1992). The zeolitic tuffs studied crop along Highway 45 between the cities of Guanajuato and Juvenile Rosa.

https://doi.org/10.1346/CCMN.1996.0440303 Published online by Cambridge University Press

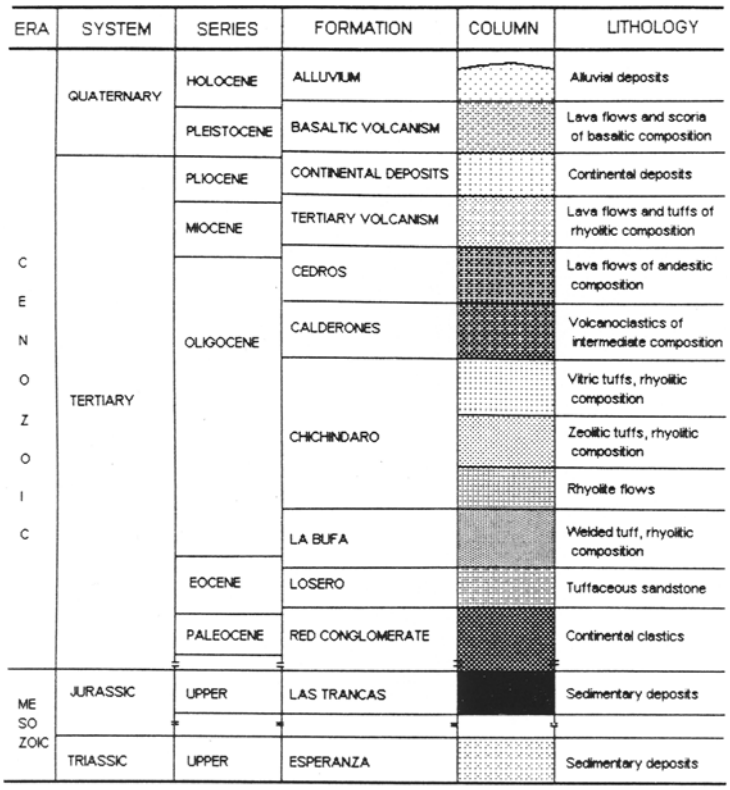

Figure 2. Stratigraphic column of the SW portion of the state of Guanajuato, with data taken from López-Ramos (1985), Nieto-Samaniego (1990) and Consejo de Recursos Minerales (1992).

Table 1. Localities, stratigraphic units and lithology of samples.

Sample	Elevation (m)	Location (km)[1]	Extension (km)[1]	Stratigraphic unit	Period	Lithology
1	1772	60.7	25.7	La Bufa	Eocene-Lower Oligocene	Welded tuff
2	1860	59.1	1.6	Chichíndaro	Oligocene	Rhyolite
3	1938	57.8	7.3	Chichíndaro	Oligocene	Rhyolite
4	1962	51.8	0	Chichíndaro	Oligocene	Zeolitic tuff
5	2035	50.4	0.9	Cedros	Oligocene-Lower Miocene	Andesite
7	2120	48.7	1.7		Quaternary	Basalt
8	2170	43.5	4.8	Chichíndaro	Oligocene	Chert
9	2174	42.3	1.6	Chichíndaro	Oligocene	Rhyolite
10	2182	42.3		Chichíndaro	Oligocene	Zeolitic tuff
	2170	40.0	2.0	Chichíndaro	Oligocene	Chert
11	2090	35.5	3.8	Chichíndaro	Oligocene	Vitric tuff
12	1995	32.9	2.6	Chichíndaro	Oligocene	Vitric tuff
13	1995	32.9		Chichíndaro	Oligocene	Zeolitic tuff
14	2010	29.3	1.7	Chichíndaro	Oligocene	Zeolitic tuff
15	2046	28.0		Chichíndaro	Oligocene	Zeolitic tuff
16	2055	28.0		Chichíndaro	Oligocene	Zeolitic tuff
17	2035	28.0	5.7	Chichíndaro	Oligocene	Zeolitic tuff
20	2040	21.2	1.5	Chichíndaro	Oligocene	Rhyolite
	2030	19.7	1.6	Chichíndaro	Oligocene	Chert
21	1920	16.6	4.1	La Bufa	Eocene-Lower Oligocene	Welded tuff
	1850	12.5	12.3	Red Conglomerate	Paleocene-Lower Eocene	Continental clastics

[1] Location and extension are given as the distance in kilometers from Guanajuato to Juventino Rosas along Highway 45.

https://doi.org/10.1346/CCMN.1996.0440303 Published online by Cambridge University Press

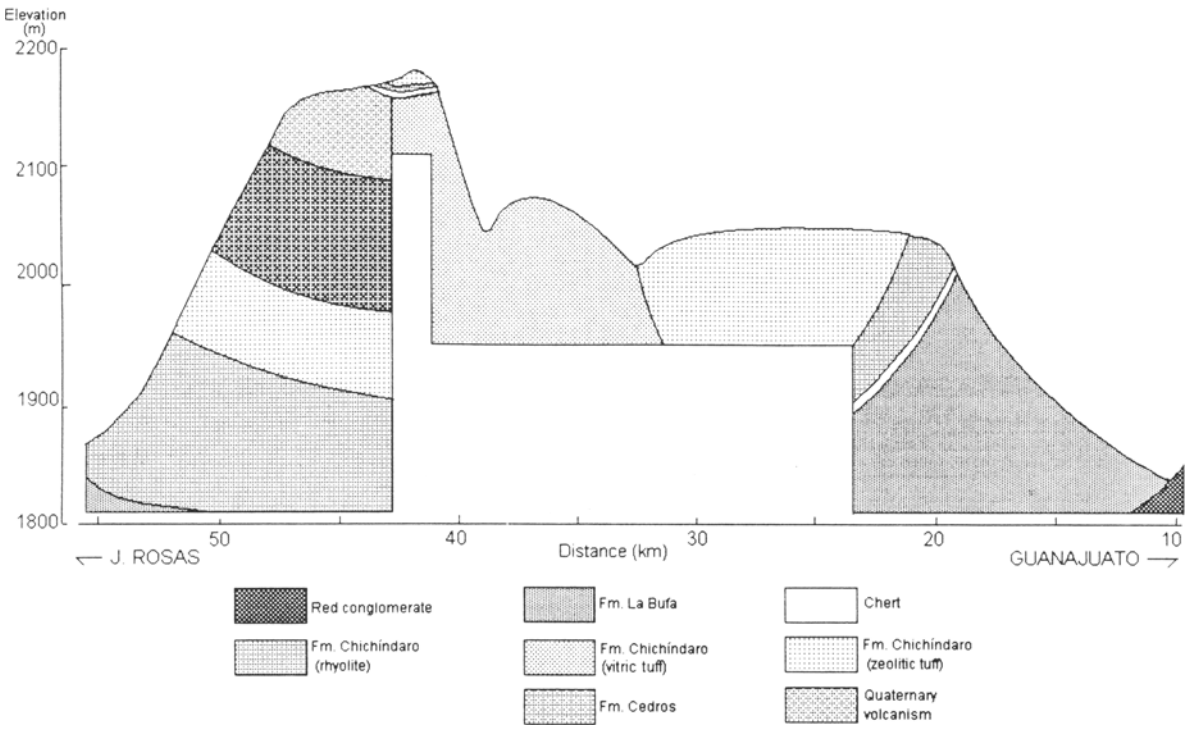

Figure 3. Schematic cross-section of the Guanajuato-J. Rosa area.

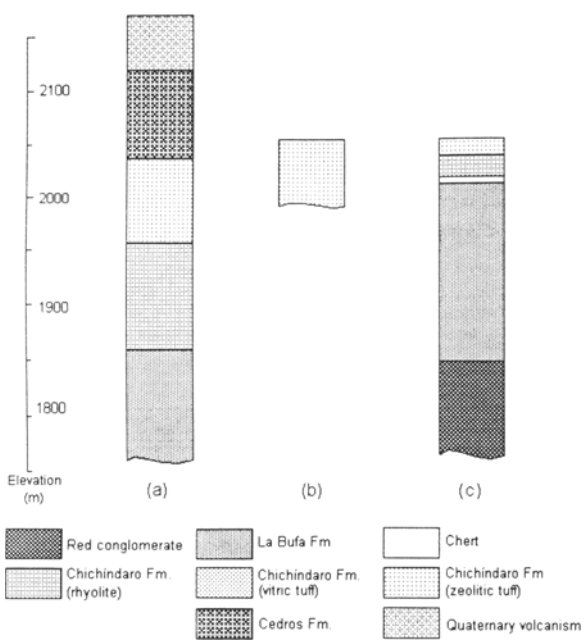

Figure 4. Schematic columnar sections of the Guanajuato-J. Rosa area: a) 50 km SW Guanajuato; b) 30 km; and c) 22 km.

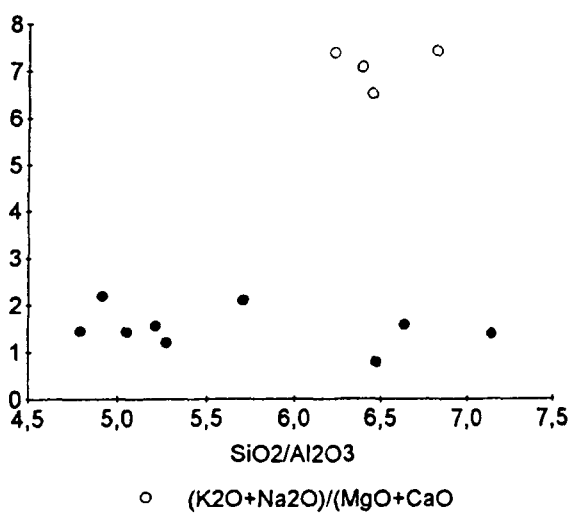

Figure 5. Variation of the ratio SiO_2/Al_2O_3 versus $(K_2O + Na_2O)/(MgO + CaO)$. The La Bufa welded tuff and the Chichíndaro rhyolite sustain SiO_2/Al_2O_3 ratios between 6.38 and 6.81 whereas the vitric and zeolitic tuffs maintain $(K_2O + Na_2O)/(MgO + CaO)$ below 2.19. Key: open circles = welded tuff and rhyolite; full circles = zeolitic tuff; and full boxes = vitric tuff.

https://doi.org/10.1346/CCMN.1996.0440303 Published online by Cambridge University Press

Table 2. Mineralogy of rocks of the La Bufa and Chichíndaro Formations.[1]

Sample	Stratigraphic unit	Lithology	Cl	Mo	Er	Sm	Op	Q	Kf	Sa	Pl	Bi	Gl
1	La Bufa	Welded tuff	—	—	—	—	30	10	20	5	—	tr	35
2	La Bufa	Rhyolite	—	—	—	5	5	40	—	40	5	5	—
3	La Bufa	Rhyolite	—	—	—	5	5	40	—	40	10	tr	—
4	La Bufa	Zeolitic tuff	60	—	—	—	5	5	—	—	—	tr	30
5	Cedros	Andesite											
7	Quaternary	Basalt											
8	Quaternary	Chert											
9	Chichíndaro	Rhyolite	—	—	—	5	—	40	—	45	10	—	—
10	Chichíndaro	Zeolitic tuff	75	—	—	—	5	—	—	—	—	—	20
11	Chichíndaro	Vitric tuff	—	—	—	30	10	5	10	—	5	—	40
12	Chichíndaro	Vitric tuff	10	—	—	25	30	5	5	tr	—	—	20
13	Chichíndaro	Zeolitic tuff	45	—	—	—	20	5	—	5	5	—	20
14	Chichíndaro	Zeolitic tuff	50	tr	tr	—	10	5	—	5	—	—	30
15	Chichíndaro	Zeolitic tuff	65	—	—	—	20	—	—	5	—	—	10
16	Chichíndaro	Zeolitic tuff	65	—	—	—	10	—	—	—	—	tr	25
17	Chichíndaro	Zeolitic tuff	60	—	—	—	10	5	—	5	5	5	10

[1] Mineralogy determined by X-ray diffraction (XRD) and microscopy. Numbers represent estimated mineral abundance in weight percent. Key: Cl = clinoptilolite; Mo = mordenite; Er = erionite; Sm = smectite; Op = opal-C; Q = quartz; Kf = K-feldspar; Sa = sanidine; Pl = plagioclase; Bi = biotite; and Gl = glass.

plays weak OH stretch vibrations that are associated with Si-OH silanol groups presumably from glass or from opal (Table 5).

CHICHÍNDARO FORMATION. The Oligocene Chichíndaro Formation is differentiated into three subunits. The lowest one is represented by the rhyolite flows that occur at an elevation of 1860 m 59.1 km SE from Guanajuato along Highway 45 and at 2170 m and 42.3 km (Figures 1 and 3; Table 1, samples 2, 3 and 9). It is brick red, fluidal, compact, dense, hypocrystalline and hypidiomorphic porphiritic with phenocrysts of quartz (40%), sanidine (40%), albite (10%) with Carlsbad law, albite twining, traces of biotite and secondary smectite (5%) (Table 2). The chemical composition is potassic with the SiO_2/Al_2O_3 and the $(Na_2O + K_2O)/(CaO + MgO)$ ratios analogous to those of the underlying welded tuff from the La Bufa Formation (Tables 3 and 4; Figure 5). The IR data indicate that this rhyolite does not contain H_2O but it has weak OH vibrations from silanol groups possibly associated with their minor contents of glass or smectite (Table 5). The rhyolite overlays chert that outcrops as a 4 m thick layer at an elevation of 2170 m 43.9 km SE from Guanajuato and at 2030 m and 19.7 km.

The vitric tuff that outcrops from 2170 to 1995 m between 40.3 to 32.9 km SE of Guanajuato (Figures 1 and 3; Table 1, samples 11 and 12) represents the second subunit of the Chichíndaro Formation. It is beige to light pink, light and coarse. Pyroclastic minerals are quartz (5%), plagioclase (<5%), with traces of sanidine. Bubble-wall glass and shards constitute 20 to 40% of the matrix. K-feldspar represented 5 to 10% and is attributed to pre-diagenetic devitrification of the glass. The tuff has been altered to smectite (30%) and

Table 3. Chemical composition of rocks.[1]

		Composition (wt %)									
Sample	Stratigraphic unit	SiO_2	Al_2O_3	TiO_2	Fe_2O_3	MgO	CaO	K_2O	Na_2O	H_2O	Total
1	La Bufa	75.46	11.40	0.11	1.10	0.74	0.30	4.60	3.10	2.66	99.8
2	Chichíndaro	75.16	11.89	0.11	1.05	0.61	0.70	5.50	3.10	1.49	99.6
3	Chichíndaro	73.47	11.81	0.11	1.34	0.76	0.50	6.30	2.50	3.05	99.8
4	Chichíndaro	68.70	12.06	0.11	1.34	0.97	1.69	4.10	1.50	8.98	99.4
9	Chichíndaro	74.13	11.61	0.17	1.62	0.45	0.70	5.80	2.50	2.70	99.8
10	Chichíndaro	64.90	13.21	0.15	1.39	1.32	1.49	5.20	0.90	10.56	99.1
11	Chichíndaro	64.75	13.29	0.53	1.36	1.49	2.19	3.50	1.80	9.93	98.8
12	Chichíndaro	68.13	13.06	0.11	1.34	1.11	1.20	2.10	1.50	10.12	98.8
13	Chichíndaro	74.26	11.19	0.10	1.05	1.29	1.49	2.80	1.50	6.22	99.9
14	Chichíndaro	74.15	10.38	0.10	1.34	0.97	2.29	3.30	1.20	6.28	100.0
15	Chichíndaro	66.27	13.11	0.17	1.39	0.99	2.29	3.60	0.90	11.15	99.9
16	Chichíndaro	69.68	10.76	0.20	1.39	1.54	2.19	2.20	0.80	11.14	99.9
17	Chichíndaro	66.88	12.70	0.13	1.34	1.59	2.29	3.40	1.20	10.30	99.8
20	Chichíndaro	74.65	11.81	0.11	1.90	0.27	0.30	4.80	3.40	2.15	99.4

[1] Analysis by X-ray fluorescence (XRF) and wet chemistry. H_2O determined by loss on ignition at 850 °C.

https://doi.org/10.1346/CCMN.1996.0440303 Published online by Cambridge University Press

Table 4. Ratios between components of rocks of the La Bufa and Chichíndaro Formations.

Sample	Stratigraphic unit	Lithology	$\frac{SiO_2}{Al_2O_3}$	$\frac{Fe_2O_3}{Al_2O_3}$	$\frac{MgO}{Al_2O_3}$	$\frac{CaO}{Al_2O_3}$	$\frac{K_2O}{Al_2O_3}$	$\frac{Na_2O}{Al_2O_3}$	$\frac{H_2O}{Al_2O_3}$	$\frac{(K_2O + Na_2O)}{(MgO + CaO)}$
1	La Bufa	Welded tuff	6.81	0.10	0.06	0.03	0.40	0.27	0.23	7.44
2	Chichíndaro	Rhyolite	6.44	0.09	0.05	0.06	0.46	0.26	0.12	6.54
3	Chichíndaro	Rhyolite	6.22	0.11	0.06	0.04	0.53	0.21	0.26	7.40
4	Chichíndaro	Zeolitic tuff	5.70	0.11	0.08	0.14	0.34	0.12	0.74	2.09
9	Chichíndaro	Rhyolite	6.38	0.14	0.04	0.06	0.50	0.21	0.23	7.10
10	Chichíndaro	Zeolitic tuff	4.91	0.10	0.10	0.11	0.39	0.07	0.80	2.19
11	Chichíndaro	Vitric tuff	4.79	0.24	0.11	0.16	0.26	0.13	0.75	1.44
12	Chichíndaro	Vitric tuff	5.21	0.10	0.08	0.09	0.16	0.11	0.77	1.58
13	Chichíndaro	Zeolitic tuff	6.63	0.09	0.11	0.13	0.25	0.13	0.55	1.58
14	Chichíndaro	Zeolitic tuff	7.14	0.13	0.09	0.22	0.32	0.11	0.60	1.39
15	Chichíndaro	Zeolitic tuff	5.05	0.11	0.07	0.17	0.27	0.07	0.85	1.42
16	Chichíndaro	Zeolitic tuff	6.47	0.13	0.14	0.20	0.20	0.07	1.03	0.79
17	Chichíndaro	Zeolitic tuff	5.27	0.10	0.12	0.18	0.27	0.09	0.81	1.20

opal-C (10%) at higher elevation and to smectite (25%), opal-C (30%) and clinoptilolite (10%) at lower altitude close to the contact with the zeolitic tuff (Table 2). Chemical data indicate that the tuff has less SiO_2 and $Na_2O + K_2O$, more Al_2O_3 and CaO + MgO, and lower SiO_2/Al_2O_3 and $(Na_2O + K_2O)/(CaO + MgO)$ ratios than the underlying rhyolite (Tables 3 and 4; Figure 5). IR analysis shows association of adsorbed H_2O and intense OH stretch vibrations (Table 5) that may correspond to smectite, glass or opal-C.

The third subunit of the Chichíndaro Formation is the zeolitic tuff that outcrops at elevations of 1962 m at 51.8 km, 2182 m at 42.3 km and 1995 to 2055 m at 32.9 to 22.3 km SE of Guanajuato (Figures 1 and 3; Table 1, samples 4, 10, 13 to 17). It is light yellowish green to gray, light, containing pyroclastic quartz (5%), sanidine (5%), plagioclase (<5%) and traces of biotite. Bubble-wall glass and shards are largely devitrified to rosettes of zeolite with about 10–30% of the glass undevitrified. The principal authigenic mineral is clinoptilolite, which represents from 45 to 75 weight% of the rock and is associated with opal-C (5–20%). Mordenite and erionite occur at an elevation of 2010 m within a silicic low Al_2O_3 bed (Table 2). The SiO_2/Al_2O_3 ratios calculated from the chemical data are between 5.05 and 7.14 and the $(Na_2O +$

Table 5. Characteristic infrared absorption vibrations.

	Wavenumber (cm^{-1})[1]													
Sample	OH stretch		H-O-H bend	Si-O-Si asymmetric stretch			Si-O-Si symmetric stretch					*Double* rings		T-O bend
1	3600	3420				1095	1035	787	720	695	640			480
	wb	wb				wsh	ib	mb	wb	w	w			m
2	3600	3420			1140		1030	785	720	695		600	525	470
	wb	wb			msh		ib	m	wb	w		m	w	m
3	3600	3420			1150		1030	792	720	695	637	600	525	470
	wb	wb			msh		ib	wb	w	w	w	m	w	m
4	3600	3420	1625	1210			1030	785	725	690	640	600		470
	m	m	m	msh			ib	i	w	w	w	m		m
10	3600	3420	1625	1200			1050	795				600	535	465
	m	m	i	wsh			ib	m				m	w	i
11	3590	3400	1625				1030	787	720	695			525	475
	i	i	i				ib	w	m	w			w	m
12	3600	3420	1625	1210			1030	787		695			528	475
	i	i	i	wsh			ib	i		w			w	m
13	3600	3420	1625	1200			1070	785	725			600	528	475
	i	i	m	wsh			ib	w	i			m	w	m
14	3600	3420	1625	1200			1050	785	725			600		470
	m	m	m	wsh			ib	i	w			m		m
15	3600	3420	1625	1200			1035	787				600	535	470
	i	i	i	wsh			ib	m				m	w	i
16	3600	3420	1625	1200			1060	785	720			600		475
	i	i	i	msh			ib	m	w			m		i
17	3600	3420	1625	1200			1050	785	725			600		470
	m	m	m	wsh			ib	m	w			m		m

[1] Vibrations are noted: w = weak; m = medium; i = intense; b = broad. Vibrations at 600 and 525 cm^{-1} are quartz.

https://doi.org/10.1346/CCMN.1996.0440303 Published online by Cambridge University Press

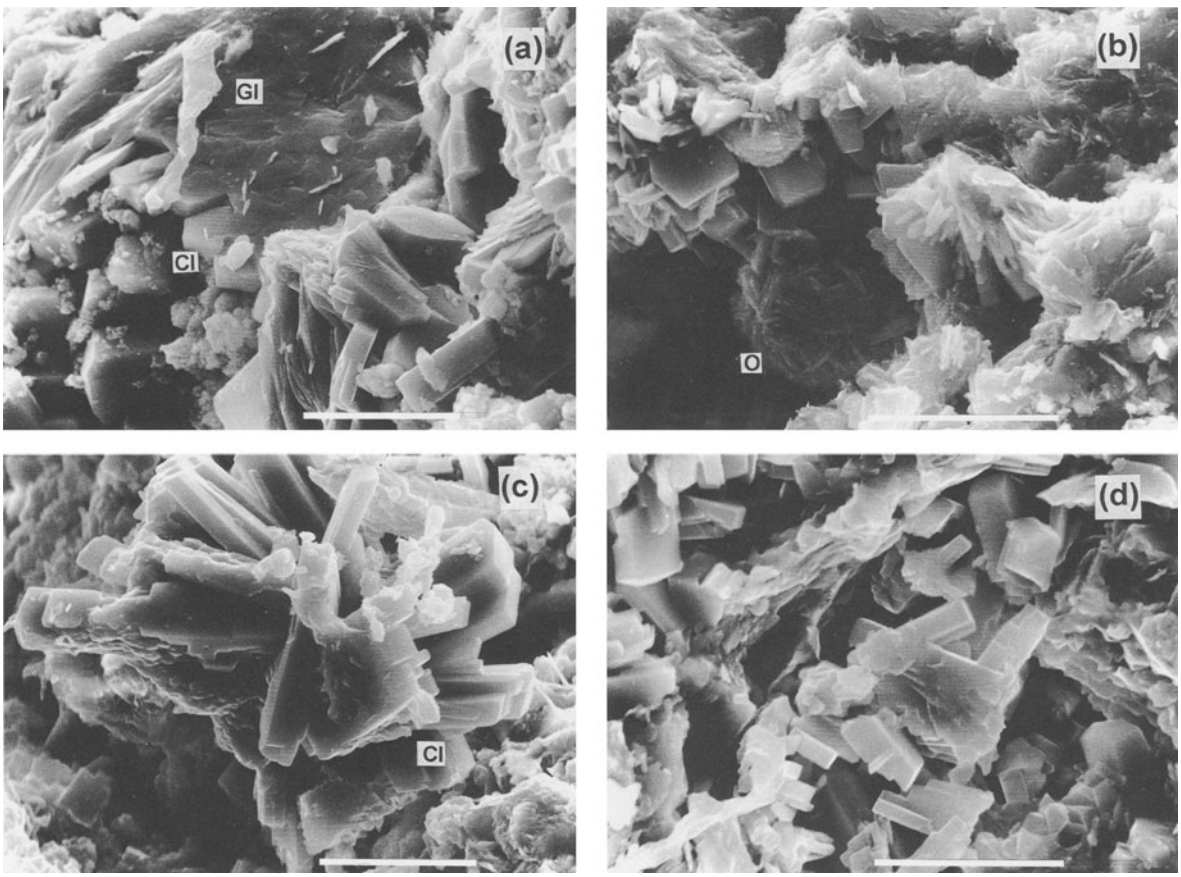

Figure 6. Scanning electron micrographs of: a) bubble-glass partially altered to block clinoptilolite, sample 15; b) bubble-glass altered to proto-zeolite and platy clinoptilolite, sample 17; c) rosette of block clinoptilolite pseudomorph after bubble-wall glass, sample 4; and d) platy and block clinoptilolite, sample 4. The horizontal bar represents 10 μm. Key: Gl = glass, Cl = clinoptilolite, Pr = proto-zeolite, O = opal-C.

K_2O)/(CaO + MgO) ratios range from 0.80 to 2.10, that are lower than those of the underlying rhyolite and cover a larger span (Tables 3 and 4; Figure 5). Their high ignition loss includes adsorbed molecular H_2O and structural OH, both confirmed by intense absorption bands from the IR (Table 5).

CEDROS FORMATION. The Upper Oligocene-Lower Miocene Cedros Formation outcrops at elevations of 2035 m 50.4 km SE of Guanajuato (Figures 1 and 3; Table 1, sample 5). It is an andesite, dark gray, hard, dense, microcrystalline, porphyritic and fluidal. It contains andesine (50%), sanidine (10%), biotite (10%), accessory quartz, olivine, hornblende, pyroxene and magnetite.

QUATERNARY VOLCANISM. The Quaternary volcanism is characterized by the basalt flows that occur at an elevation of 2120 m 48.7 km SE of Guanajuato (Figures 1 and 3; Table 1, sample 7). It is an olivine basalt, dark gray, hard, dense and microcrystalline. Its mineralogical assemblage is anorthite (50%), augite (10%), olivine (10%) and accessory magnetite, hematite and apatite.

Authigenic Mineralogy

The authigenic minerals are clinoptilolite, mordenite, erionite, opal-C, K-feldspar, smectite and quartz.

ZEOLITE MINERALS. Clinoptilolite occurs as well-formed platy and block crystals that are from 7 to 10 μm long and 3 to 5 μm wide. It replaces glass and is evenly distributed throughout the zeolitic tuff of the Chichíndaro Formation (Figure 6). It is the principal mineral representing from 45 to 75% weight of the tuff. It is associated with an estimated 25% unaltered glass, 10% opal-C and 8% of pyroclastic quartz, sanidine, albite and biotite. It does not occur within the welded tuff of the La Bufa Formation. In the vitric tuff unit of the Chichíndaro Formation, it appears only as a minor constituent and is associated with smectite and opal-C from material collected close to the contact with the zeolite tuff. SEM data indicate that clinoptilolite is

https://doi.org/10.1346/CCMN.1996.0440303 Published online by Cambridge University Press

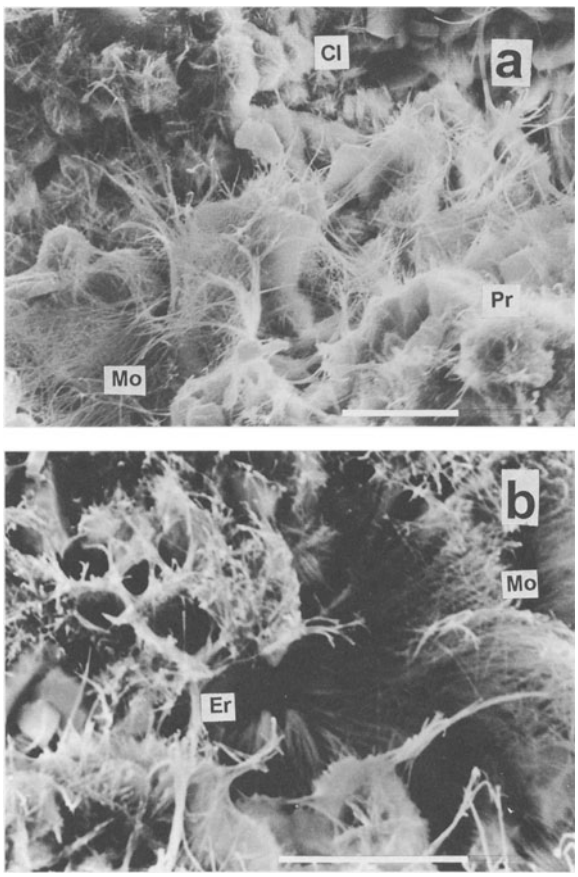

Figure 7. Scanning electron micrographs of: a) mordenite fibers associated with clinoptilolite; and b) mordenite fibers pseudomorph after bubble-wall glass and erionite fibers, sample 14. The horizontal bar represents 10 μm. Key: Mo = mordenite; Cl = clinoptilolite; Pz = proto-zeolite; and Er = erionite.

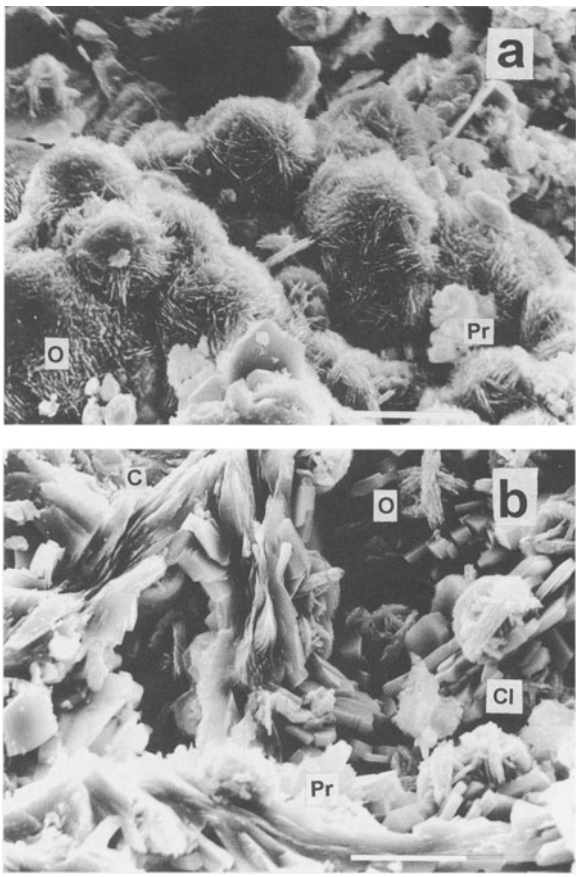

Figure 8. Scanning electron micrographs of: a) opal-C associated with platy clinoptilolite and proto-zeolite, sample 13; and b) crystal blades of cristobalite associated with clinoptilolite and proto-zeolite, sample 17. The horizontal bar represents 10 μm. Key: O = opal-C; Cl = clinoptilolite; C = cristobalite; and Pz = proto-zeolite.

also formed from a proto-zeolite precursor. The precursor appears as irregular vitreous parallel or radiating lamellae that often terminate as straight edges and is associated with crystallites of clinoptilolite (Figures 6b, 7, and 8b).

This clinoptilolite is stable to 500 °C with only minor reduction in the intensity of the diffraction peaks. The composition (Table 6), determined by EDX, calculated for a 72 oxygen cell (Breck 1974; Alberti 1975; Alieti 1972) corresponds to the formula:

$$(Si_{0.99}Al_{0.01}O_2)_{30}(Al_{1.09}Fe_{0.01}O_2)_6(Na_{0.07}K_{0.34}Ca_{0.10}Mg_{0.07})_6 \times H_2O$$

Mordenite occurs in the form of thin fibers less than 0.5 μm in diameter and 15 μm long. It is associated with clinoptilolite and erionite from the tuff occurring at an elevation of 2010 m (Table 1, sample 14). Some fibers appear to be pseudomorphic after bubble-wall glass (Figure 7). The composition of the mineral (Table 6) calculated to a 72 oxygen cell conforms to the formula:

$$(Si_{0.99}Al_{0.01}O_2)_{30}(Al_{1.02}Fe_{0.04}O_2)_6(Na_{0.09}K_{0.14}Ca_{0.18}Mg_{0.14})_6 \times H_2O.$$

The Si/Al ratio is 4.88 and is higher than the 4.51 value obtained for clinoptilolite. SEM studies indicate that this mordenite may have crystallized both from solutions and from glass rather than from precursor clinoptilolite.

Erionite occurs as a thick fibrous mineral associated with mordenite and clinoptilolite from the zeolitic tuff at an elevation of 2010 m (Figure 7).

Opal-C spheres about 10 μm in diameter and blades of cristobalite embedded in glass from the zeolitic tuff are conspicuous from the SEM studies (Figures 6 and 8). It is also an important constituent of the vitric tuff where it is associated with smectite. In the welded tuff of the La Bufa Formation, it was devitrified from glass

https://doi.org/10.1346/CCMN.1996.0440303 Published online by Cambridge University Press

Table 6. Chemical composition of unaltered glass and diagenetic minerals.[1]

	Glass	Clinoptilolite		Mordenite	Opal-C
		Chemical composition (%)			
SiO_2	77.42	78.27	77.69	76.70	78.57	97.35
Al_2O_3	13.10	14.73	14.44	14.45	13.67	1.21
TiO_2	0.08	0.08	0.18	0.07	0.07	0.04
Fe_2O_3	3.26	0.25	0.25	0.96	0.87	0.28
MnO	0.05	0.07	0.05	0.06	0.07	0.04
MgO	0.81	0.75	0.83	0.86	1.52	0.17
CaO	1.65	2.42	2.69	1.79	2.71	0.23
K_2O	3.08	2.89	3.58	4.41	1.76	0.20
Na_2O	0.55	0.54	0.29	0.69	0.76	0.48
Total	100.00	100.00	100.00	99.99	100.00	100.00
		Unit-cell contents			
Si		29.83	29.78	29.56	29.89	
Al		6.61	6.51	6.55	6.12	
Ti		0.02	0.05	0.02	0.02	
Fe		0.07	0.07	0.28	0.25	
Mg		0.42	0.47	0.49	0.86	
Ca		0.99	1.10	0.74	1.10	
K		1.41	1.75	2.17	0.85	
Na		0.40	0.21	0.51	0.56	
O		72	72	72	72	
Si/Al		4.51	4.57	4.51	4.88	
Si/(Al + Ti + Fe)		4.45	4.49	4.31	4.68	

[1] Chemical analysis by energy dispersive X-ray coupled to scanning electron microscopy. Values in weight percent, dry basis. Fe assumed as Fe_2O_3. Unit-cell contents based on 72 O atoms.

and appears with K-feldspar. Its chemical composition indicates that it retains minor concentrations of Al, Fe and alkali ions, which could also be in the form of intimately associated glass (Table 6).

Approximately 5% smectite occurs in the rhyolite and 20–25% in the vitric tuff. It is associated with opal-C or with opal-C + clinoptilolite (sample 12). It is not found in the zeolitic tuffs. It is characterized by a weak (001) reflection at 15.5 Å, which expands to 17.5 Å upon solvation. The (060) reflection at 1.495 Å is weak and broad, which corresponds to a dioctahedral smectite.

Cryptocrystalline K-feldspar is identifiable from the devitrified bubble-wall glass and shards within the welded tuff and the vitric tuff, which are different from the pyroclastic sanidine phenocrysts common to these rocks and is interpreted as authigenically formed.

Bubble-wall glass and shards are unaltered, pitted or partially altered to clinoptilolite, mordenite and erionite (Figures 6, 7, 8 and 9). The bubble wall glass and shards concentrations range from 10 to 40%. They have a refractive index below 1.51 and a composition that corresponds to a rhyolitic glass (Table 6).

Quartz occurs authigenic within the vitric and zeolitic tuffs. It is characterized by its saccaroidal microtexture and undulatory extinction, which is distinct from pyroclastic quartz.

DISCUSSION

Diagenetic Facies

Two different lithologic units are considered in the discussion of the diagenetic facies. One, which does not correspond properly to a diagenetic facies, is represented by the welded tuff of the La Bufa Formation that contains pyroclastic quartz, sanidine, a minor quantity of biotite and rhyolitic glass devitrified to K-feldspar + opal-C. The unit depicts a pre-diagenetic process of devitrification, prior to the diagenetic changes that occurred within the overlying Chichíndaro Formation. The absence of water and diagenetic smectite or zeolite from the La Bufa Formation confirms a mechanism of devitrification rather than a process of diagenetic alteration.

The second lithologic unit is the Chichíndaro Formation with its rhyolitic, vitric tuff, and zeolitic tuff subunits. In the rhyolite, glass appears slightly altered to smectite + opal-C. This indicates minor diagenesis within a lacustrine environment and defines the sequence rhyolitic glass → smectite + opal-C. In the vitric tuff, glass is equally transformed to smectite + opal-C with some K-feldspar resulting from pre-diagenetic devitrification. Close to the contact with the zeolitic tuff, the association of minor clinoptilolite with smectite is attributed to microenvironmental changes rather than to a transformation from one into the other. In the zeolitic tuff, principal clinoptilolite resulting from the reactions rhyolitic glass → clinoptilolite + mordenite + erionite + opal-C and rhyolitic glass → clinoptilolite + opal-C.

Paragenesis of Diagenetic Minerals

The sequences of crystallization are: 1) rhyolitic glass → K-feldspar + opal-C; 2) rhyolitic glass →

https://doi.org/10.1346/CCMN.1996.0440303 Published online by Cambridge University Press

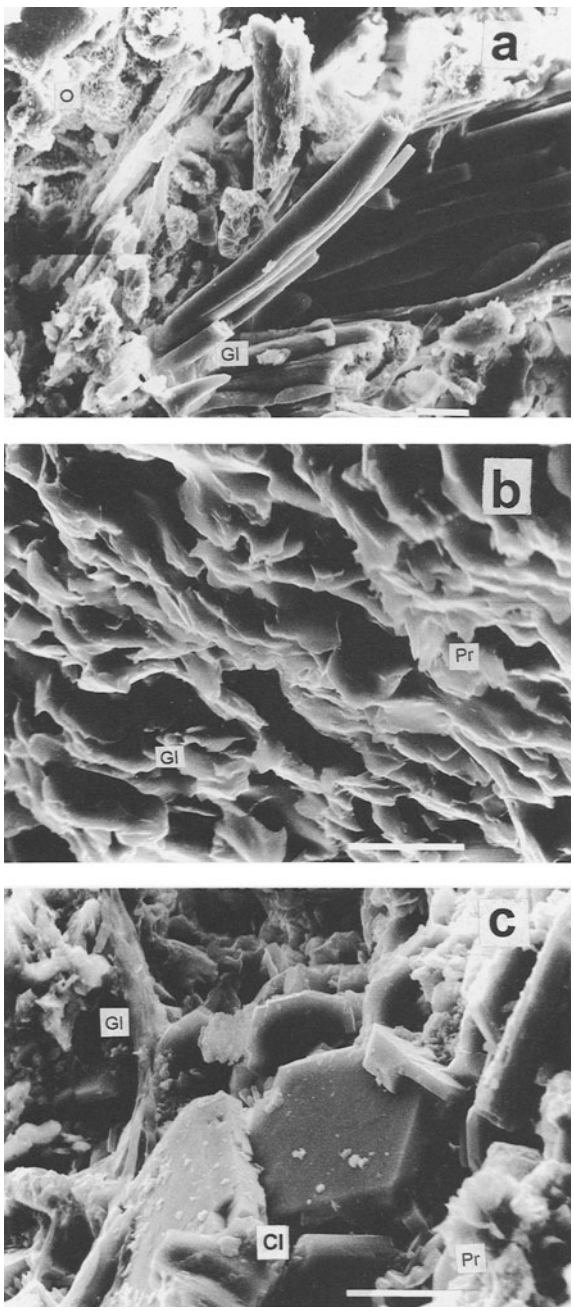

Figure 9. Scanning electron micrographs of: a) unaltered glass rods; b) glass transformed into irregular parallel vitreous lamellae of proto-zeolite; and c) altered and pitted glass and clinoptilolite. Sample 10. The horizontal bar represents 10 μm. Key: Cl = clinoptilolite; Pz = proto-zeolite; and Gl = glass.

smectite + opal-C; 3) rhyolitic glass → clinoptilolite + opal-C; and 4) rhyolitic glass → clinoptilolite + mordenite + erionite + opal-C. Similar sequences have been identified from other sedimentary deposits (Surdam 1977; Hay and Sheppard 1977; Altaner and Grim 1990; Sheppard 1991). The first reaction corresponds to a process of devitrification of glass from the precursor ash fall. The other reactions depict diagenetic events under normal atmospheric conditions. Alteration of a rhyolitic precursor at high temperature and water vapor pressure under a "geoautoclave" effect does not appear to have formed in the present case.

Geochemistry of Zeolite Diagenesis

The data presented indicates that the zeolitic and vitric tuffs were formed from a precursor ash fall of rhyolitic composition. The most stable components for this zeolite system are Al_2O_3, which averages 11.77% for the rhyolite, 13.17 for the vitric tuff, and 11.91% for the zeolitic tuff. The Fe_2O_3 content is 1.34%, which is nearly equal for the three units and confirms the alkaline diagenetic environment. The relations between the various components and Al_2O_3 readily discriminate the welded tuff of the La Bufa Formation and the overlying rhyolite of the Chichíndaro Formation from the vitric and zeolitic tuffs of the Chichíndaro Formation (Figure 10). The data show that these two units are chemically alike and that the tuffs have about equal Fe_2O_3, less SiO_2, K_2O and Na_2O and more MgO, CaO and H_2O than their rhyolitic precursor (Figure 11). In the zeolitic tuff, clinoptilolite forms at compositions changing from 10.38 to 13.21% Al_2O_3 and between 74.15–64.90% SiO_2, 0.97–1.59% MgO, 2.29–1.49% CaO, 2.20–5.20% K_2O, 0.80–1.50% Na_2O, 1.34% Fe_2O_3 and 6.28–10.56% H_2O. Essentially linear correlations occur between Al_2O_3 and the remaining constituents. Low Al_2O_3 clinoptilolite-containing tuff is associated with high SiO_2, MgO and CaO, and low K_2O, Na_2O and H_2O contents whereas high Al_2O_3 clinoptilolite tuff has low SiO_2, MgO and CaO, and high Na_2O, K_2O and H_2O contents (Figure 10).

The vitric tuff contains 65.94% SiO_2 and the zeolite tuff 69.55%, which is less than the 74.33% of the rhyolite. The CaO changes threefold from an average of 0.63% for the rhyolite to 1.69% for the vitric tuff and 1.96% for the zeolitic tuff. The MgO increases from 0.61% to 1.30% and 1.24%. The K_2O decreases from 5.86% to 2.80% and 3.51% and the Na_2O from 2.70% to 1.65% and 1.14%. The SiO_2/Al_2O_3 and SiO_2/Fe_2O_3 ratios are lower and Al_2O_3/Fe_2O_3 higher for the vitric tuff than for the zeolitic. The MgO/Al_2O_3 and MgO/Fe_2O_3 and CaO/Al_2O_3 and CaO/Fe_2O_3 are approximately equal for both tuffs, two to three times higher than for the rhyolite. The K_2O/Al_2O_3 and K_2O/Fe_2O_3 and Na_2O/Al_2O_3 and Na_2O/Fe_2O_3 ratios are about the same and approximately half of what they are in rhyolite.

The change from the rhyolitic precursor to the zeolitic tuff is more sensitive to SiO_2 and less to the other

https://doi.org/10.1346/CCMN.1996.0440303 Published online by Cambridge University Press

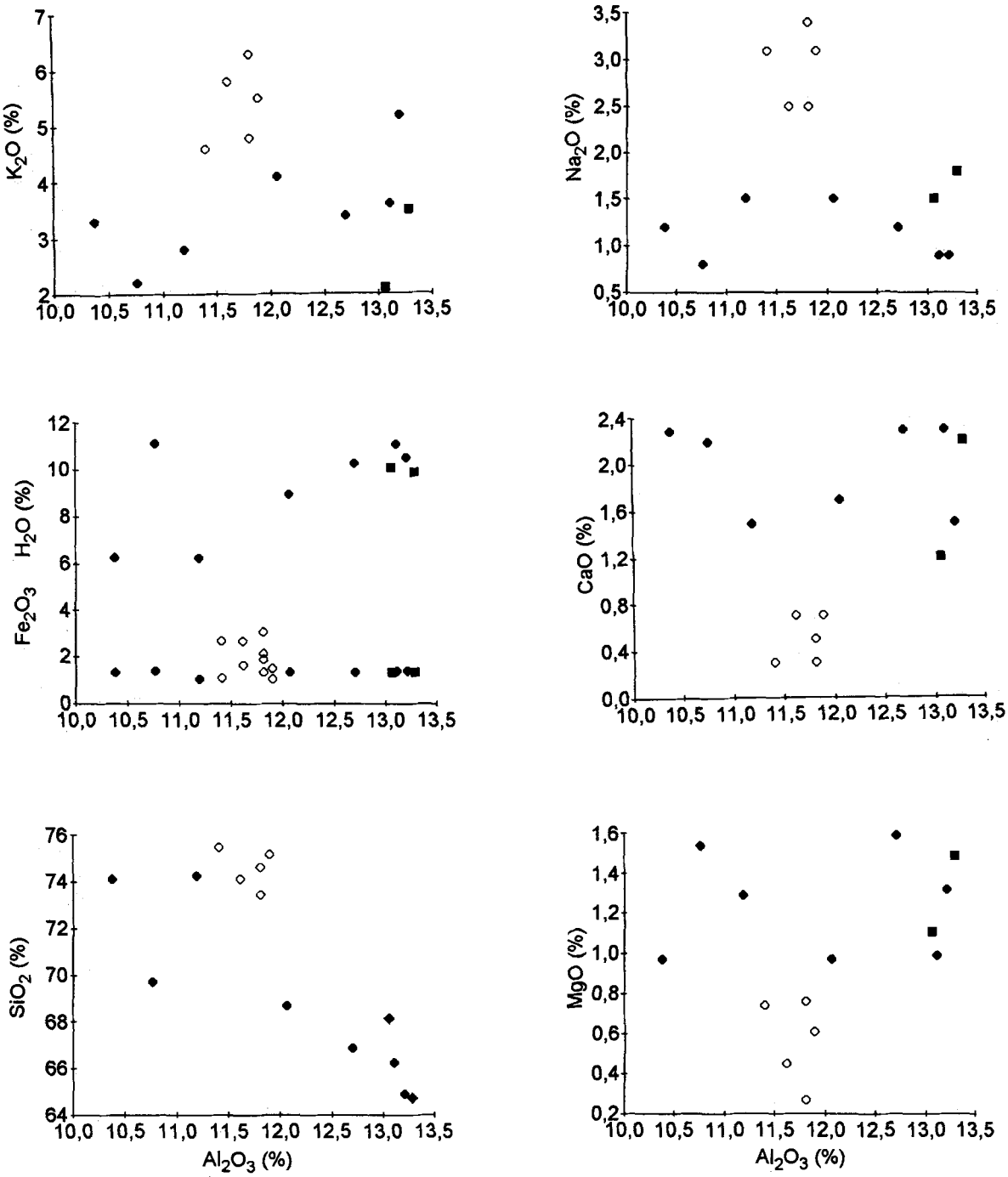

Figure 10. Variation in chemical composition versus Al_2O_3 in rocks from the La Bufa and Chichíndaro Formations. Key: Open circles = welded tuff and rhyolite; full circles = zeolitic tuff; and full boxes = vitric tuff.

constituents making the process one of hydration and desilication. The XRD patterns depict that the formation of clinoptilolite from the rhyolitic precursor for this system is associated with: 1) reduction of the contents of SiO_2 and proportional enrichment of Al_2O_3 while Fe_2O_3 stays essentially constant; 2) reduction of K_2O and Na_2O and increase of MgO, CaO and H_2O or the inverse behavior of Na_2O and K_2O relative to MgO and CaO; 3) compositional SiO_2/Al_2O_3 ratios between the limits 4.91 to 7.14 and $(K_2O + Na_2O)/(MgO + CaO)$ ratios from 2.19 to 0.79. The compositions of clinoptilolite and mordenite (Table 6) with relatively

https://doi.org/10.1346/CCMN.1996.0440303 Published online by Cambridge University Press

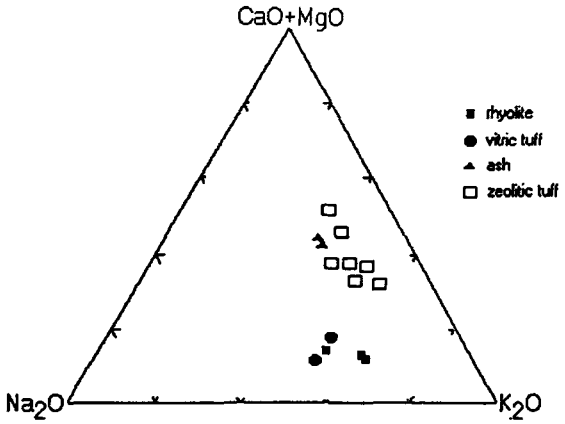

Figure 11. Composition of welded tuff of the La Bufa Formation and rhyolite, vitric and zeolitic tuffs of the Chichíndaro Formation in the system Na_2O-(CaO + MgO)-K_2O.

high contents of K_2O and CaO confirm high activities for these elements (Hay and Sheppard 1977; Bowers and Burns 1990). The sequence of crystallization clinoptilolite-mordenite-erionite may imply a local, more alkaline environment (Mariner and Surdam 1970; Sheppard 1991). Clinoptilolite forms directly from the rhyolitic bubble glass and shards, and from a "proto-zeolite" vitreous intermediate phase.

The zeolitic tuff contains opal-C from 5% for the most zeolitized material to 20% for the least one. This opal-C accommodates 0.20% K_2O and 0.48% Na_2O in its structure (Table 6). The contents of opal and alkalis associated with zeolite appear to be less than expected from the desilication of the rhyolitic precursor. Consequently, some must have been lost from the system. This, associated with the absence of smectite in the zeolite tuff, leads to conclude that diagenesis was in an open hydrologic system.

The vitric tuff has more Al_2O_3, MgO and Na_2O, and less SiO_2, CaO and K_2O, and equal Fe_2O_3, than the zeolitic tuff. The diagenesis follows the same patterns as that for zeolite (Figures 10 and 11). The data depict diagenetic alteration to smectite and opal-C from a closed lacustrine environment of different alkalinity. The association of K-feldspar from devitrified glass and the coarser texture of the vitric tuff point toward additional devitrification and possible differences in hydrology.

The role of H_2O in the formation of zeolites is well-known (Hay 1966, 1977; Surdam 1977; Lander and Hay 1993). Infrared absorption studies show that the H-O-H bending frequency of the H_2O molecule at 1625 cm^{-1} does not occur for the welded tuff of the La Bufa Formation or the Chichíndaro rhyolite. Whereas, for the vitric tuff and the zeolitic tuff, it appears intense and well-defined. The data support that diagenesis did not occur within the La Bufa Formation and that embodied K-feldspar and opal-C resulted from devitrification of the rhyolitic glass. For the rhyolite, devitrification did not take place but there was very minor diagenesis that resulted in the formation of smectite. Much to the contrary, the IR data confirm that H_2O was essential for the alteration of the glass and crystallization of smectite and clinoptilolite from the vitric and zeolitic tuffs.

For the OH-stretch region, H-bonded OH stretch occurs at 3600 and 3420 cm^{-1} weak and broad for the welded tuff and rhyolite and intense for the vitric and zeolitic tuffs. They imply structural silanol Si-OH groups for opal-C and glass from the welded and vitric tuffs for smectite and zeolite from the latter. This is confirmed by the intense (SiSi)O-OH and weak (SiAl)O-OH vibrations at 787 and 720 cm^{-1}. They are not assigned to octahedral Al-OH-Al, Al-OH-Mg or Al-OH-Fe groups because the Al-OH-Al bending vibrations at 822 and 755 cm^{-1} or the Mg-OH-Mg bending vibrations at 670 and 650 cm^{-1}, were not identified from the present samples (Farmer 1974; Shirozu 1980; Bergaya et al. 1985; Shirozu and Ishida 1982).

The Si-O-Si asymmetric stretch at 1095 and 1035 cm^{-1} from the welded tuff and at 1140 and 1030 cm^{-1} from the rhyolite coincide with the vibrations that typify quartz (Salisbury et al. 1991). For the zeolitic tuff, the stretch occurs at 1060 cm^{-1} and at 1030 cm^{-1} for the vitric tuff. The vibrations at 1095 and 1035 cm^{-1}, characteristic of Al-O and Si-O for the welded tuff, are displaced to 1060 cm^{-1} for the zeolitic tuff pointing to predominance of tetrahedral Si groups over tetrahedral Al groups and no octahedral. Si-O-Si symmetric stretch is represented by vibrations at wavelengths from 792 to 637 cm^{-1}, which are insensitive to structural variations. Vibrations assigned to double 4- and 6-rings reported to occur for some zeolites in the range 650 to 500 cm^{-1} (Breck 1974) are displaced for the present case and occur in the rhyolite as well. Those vibrations recorded at 1200, 1050, 910, 785, 725, 597, 535 and 475 cm^{-1} have been assigned to mordenite, heulandite and clinoptilolite (Salisbury et al. 1991).

CONCLUSIONS

A sizable deposit of clinoptilolite in the form of zeolitic tuff containing an average 65% of the mineral, which may have economic significance for certain applications, has been located within the limits of the Mexican Volcanic Belt with the Mexican Highlands in the state of Guanajuato, Mexico.

The zeolitic tuff represents the upper limit of the Oligocene Chichindaro Formation. Clinoptilolite is the principal zeolite and is associated with mordenite and erionite in one particular location. They were formed by diagenetic alteration of rhyolitic ash falls from an open hydrologic environment. The zeolitic tuff is in contact with a vitric tuff where devitrification of the ash formed minor K-feldspar, and posterior diagenesis

resulted into smectite and opal-C for a lacustrine setting. The Chichíndaro Formation overlies the welded tuff of the Eocene-Oligocene La Bufa Formation where rhyolitic glass appears devitrified to K-feldspar + opal-C. The diagenetic facies are: 1) smectite + opal-C; 2) clinoptilolite + opal-C; and 3) clinoptilolite + mordenite + erionite + opal-C.

The alteration of rhyolitic glass to clinoptilolite, mordenite and erionite is associated with reduction of SiO_2, K_2O and Na_2O, proportionally increasing the contents of Al_2O_3, MgO, CaO and H_2O, Fe_2O_3 remains constant. Part of the SiO_2 removed from the glass is in the form of NaK-containing opal-C associated with the zeolite. When the alteration was to smectite, higher concentrations of opal-C and chemical constituents remained associated with smectite. Formation of zeolite appears to occur when the ratio SiO_2/Al_2O_3 is between 4.91 and 7.14 and the ratio $(K_2O + Na_2O)/(MgO + CaO)$ remains from 2.19 to 0.79. Infrared absorption data confirms that diagenesis is a process of hydration on the rhyolitic glass.

ACKNOWLEDGMENTS

The authors are indebted to the Programa de Apoyo a Proyectos de Investigación e Innovación Tecnológica, of the Universidad Nacional A. de México for its financial support to project IN106994. Appreciation is manifested to A. Lozano, A. Maturano and M. Reyes for their participation with the analytical work.

REFERENCES

Alberti A. 1975. The crystal structure of two clinoptilolites. Tschermak Mineral Petrog Mitt 22:35–37.

Alieti A. 1972. Polymorphism and crystal chemistry of heulandites and clinoptilolites. Am Mineral 57:1448–1462.

Altaner SP, Grim RE. 1990. Mineralogy, chemistry, and diagenesis of tuffs in the Sucker Creek Formation (Miocene), Eastern Oregon. Clays & Clay Miner 38:561–572.

Bergaya F, Brigati MF, Fripiat JJ. 1985. Contribution of infrared spectroscopy to the study of corrensite. Clays & Clay Miner 33:458–462.

Boles JR. 1972. Composition, optical properties, cell dimensions, and thermal stability of some heulandite group zeolites. Am Mineral 57:1463–1493.

Bowers TS, Burns RG. 1990. Activity diagrams for clinoptilolite: Susceptibility of this zeolite to further diagenetic reactions. Am Mineral 75:601–619.

Breck DW. 1974. Zeolite molecular sieves. Structure, chemistry, and uses. New York: Wiley. 771 p.

Comisión de Estudios del Territorio Nacional. 1973a. Carta Geológica F-14-C-52, Escala 1:50000. Secretaría de la Presidencia, México. Map.

Comisión de Estudios del Territorio Nacional. 1973b. Carta Geológica San Miguel Allende F-14-C-54, Escala 1:50000. Secretaría de la Presidencia, México. Map.

Comisión de Estudios del Territorio Nacional. 1973c. Carta Geológica Guanajuato F-14-C-53, Escala 1:50000. Secretaría de la Presidencia, México. Map.

Consejo de Recursos Minerales. 1992. Monografía geológico minera del Estado de Guanajuato. México. 1–60.

de Cserna-Gombos Z. 1975. On the geology of parts of the Trans-Mexican Volcanic Belt and of the Mexican Central Plateau. In:de Pablo L, editor. Field Trip FT-1 Guidebook, 1975 International Clay Conference. Instituto de Geologia, Universidad Nacional A. de México, México. 72 p.

de Pablo-Galán L. 1979. The clay deposits of Mexico. In: Mortland MM, Farmer VF, editors. Proceedings International Clay Conference 1978. Amsterdam: Elsevier. p 475–486.

de Pablo-Galán L. 1986. Geochemical trends in the alteration of Miocene vitric tuffs to economic zeolite deposits, Oaxaca, Mexico. Applied Geochemistry 1:273–285.

Echegoyen-Sánchez J. 1970. Geologia y yacimientos minerales de la parte central del distrito minero de Guanajuato. Consejo de Recursos Naturales No Renovables, México. Boletín 75:1–36.

Farmer VC. 1974. The infrared spectra of minerals. London: Mineralogical Society. 539 p.

Gonzalez-Sandoval JR. 1987. Geología del depósito de zeolitas de El Cajón, Mpio. de Rayón, Sonora. In: II Conferencia Nacional Sobre Zeolitas, Hermosillo. Resúmen de Ponencias. Hermosillo, Mexico. 19 p.

Hay RL. 1963. Stratigraphy and zeolite diagenesis in the John Day Formation of Oregon. Univ California Publ Geol Sci 42:199–262.

Hay RL. 1966. Zeolites and zeolitic reactions in sedimentary rocks. Geol Soc Am Spec Pap 85:1–130.

Hay RL. 1977. Geology of zeolites in sedimentary rocks. In: Mumpton FA, editor. Mineralogy and geology of natural zeolites. Mineral Soc Am Rev Mineral Vol. 4:53–64.

Hay RL. 1978. Geologic occurrence of zeolites. In: Mumpton FA, Sand LB, editors. Natural zeolites. Oxford: Pergamon Press. p 135–143.

Hay RL, Sheppard RA. 1977. Zeolites in open hydrologic systems. In:Mumpton FA, editor. Mineralogy and geology of natural zeolites. Mineral Soc Am Rev Mineral Vol. 4: 93–102.

Lander RH, Hay RL. 1993. Hydrogeologic control on zeolitic diagenesis in the White River sequence. Geol Soc Am Bull 105:361–376.

López-Ramos Ernesto. 1985. Geología de México. Mexico II:403–445.

Mariner RH, Sordam RC. 1970. Alkalinity and formation of zeolites in saline alkaline lakes. Science 170:977–980.

Minato H, Namba H, Iton N. 1985. Thermal behaviour of clinoptilolite. Part 1. Hyogo Univ Teacher Educ J:101–112.

Mumpton FA. 1960. Clinoptilolite redefined. Am Mineral 45:351–369.

Mumpton FA. 1973. First reported occurrence of zeolites in sedimentary rocks of Mexico. Am Mineral 58:287–290.

Mumpton FA. 1975. Zeolitic tuffs in the vicinity of Oaxaca. In:de Pablo L, editor. Field trip guide book. International Clay Conference. Instituto de Geologia, Universidad Nacional A. de México, México. 45–57.

Mumpton FA. 1977. Utilization of natural zeolites. In: Mumpton FA, editor. Mineralogy and geology of natural zeolites. Mineral Soc Am Rev Mineral Vol. 4:177–204.

Nieto-Samaniego AF. 1990. Fallamiento y estratigrafia Cenozoicos en la parte sudoriental de la Sierra de Guanajuato, Revista Instituto de Geologia 9:145–155.

Ortega F, Mitre LM, Roldan J, Aranda J, Moran D, Alniz S, Nieto D. 1992. Carta geologica de la Republica Mexicana. Ed. Instituto de Geologia, Universidad Nacional A. de Mexico, Mexico.

Salisbury JW, Walter LS, Vergo N, D'Aria DM. 1991. Infrared (2.1–25 mm) spectra of minerals. Baltimore: Johns Hopkins University Press. 267 p.

Samaniego S. 1987. Geología del depósito de zeolitas El Alamo. Mpio. de Agua Prieta, Sonora. In: II Conferencia Nacional Sobre Zeolitas. Hermosillo. Resúmen de Ponencias. Hermosillo, México. 19 p.

Sheppard RA. 1991. Zeolitic diagenesis of tuffs in the Miocene Chalk Hills Formation, Western Snake River Plain, Idaho. US Geol Surv Bull. 27 p.

Shirozu H. 1980. Cation distribution, sheet thickness, and O-OH space in trioctahedral chlorites: An X-ray and infrared study. Japan. Mineral J 10:14–34.

Shirozu H, Ishida K. 1982. Infrared study of some 7A and 14A layer silicates by deuteration. Japan. Mineral J 11: 161–171.

Surdam RC. 1977. Zeolites in closed hydrologic systems. In: Mumpton FA, editor. Mineralogy and geology of natural zeolites. Mineral Soc Am Rev Mineral Vol. 4:65–91.

Tsolis-Katagas P, Katagas C. 1989. Zeolites in pre-caldera pyroclastic rocks of the Santorini volcano, Aegean Sea, Greece. Clays & Clay Miner 37:497–510.

Walton AW 1975. Zeolitic diagenesis in Oligocene Volcanic sediments, Trans-Pecos Texas. Geol Soc Am Bull 86:615–624.

Wilson JA, Clabaugh SE. 1970. A new Miocene Formation and a description of volcanic rocks, Northern Valley of Oaxaca. In: Segura LR, Rodriguez R, editors. Libro guia de la excursión México-Oaxaca. Sociedad Geológica Mexicana. p 120–128.

(Received 25 January 1995; accepted 31 July 1995; Ms. 2614)